Jet spectra in FRI radio galaxies: implications for particle acceleration

R.A. Laing (ESO), A.H. Bridle, W.D. Cotton (NRAO), D.M. Worrall, M. Birkinshaw (U. Bristol)

1 Introduction

The detection of X-ray synchrotron emission on kiloparsec scales in the bases of low-luminosity (FR I) radio jets (e.g. [2, 3, 13]) requires distributed particle acceleration, consistent with the failure of adiabatic models to reproduce the observed brightness profiles at radio wavelengths [6]. The acceleration mechanism is not understood. We present very precise imaging of spectral variations at radio wavelengths which suggest that the character of the acceleration process changes both along and across the jets. We relate these changes to our models of jet kinematics and suggest that deceleration and velocity shear are both important in determining the spectrum. We also present a new, deep *Chandra* image of the brighter jet in NGC 315 and use it to demonstrate an association between the X-ray/radio emission ratio and the jet kinematics.

2 NGC 315

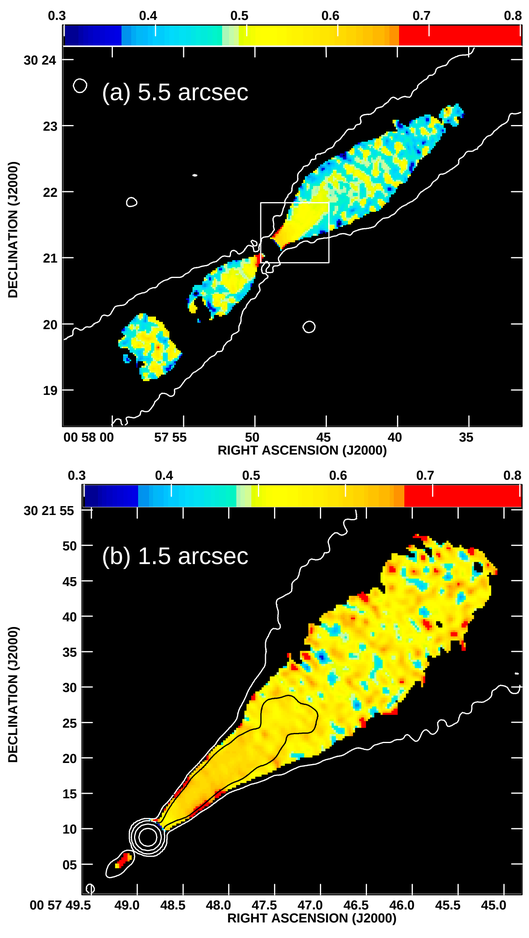

Figure 1: (a) False-colour plots of spectral index, α over the range 0.3 – 0.8 for NGC 315 [7]. (a) α determined by weighted power-law fits to data at five frequencies between 1.365 and 5 GHz. The resolution is 5.5 arcsec FWHM. (b) α between 1.413 and 5 GHz at a resolution of 1.5 arcsec FWHM.

Figure 2: Overlays of VLA 5 GHz images (contours) on adaptively smoothed *Chandra* 0.8 – 5 keV data (colour) for NGC 315 [13]. (a) Radio resolution 1.5 arcsec. The area covered by panel (b) is shown by the white box. (b) radio resolution 0.4 arcsec.

3 3C 31

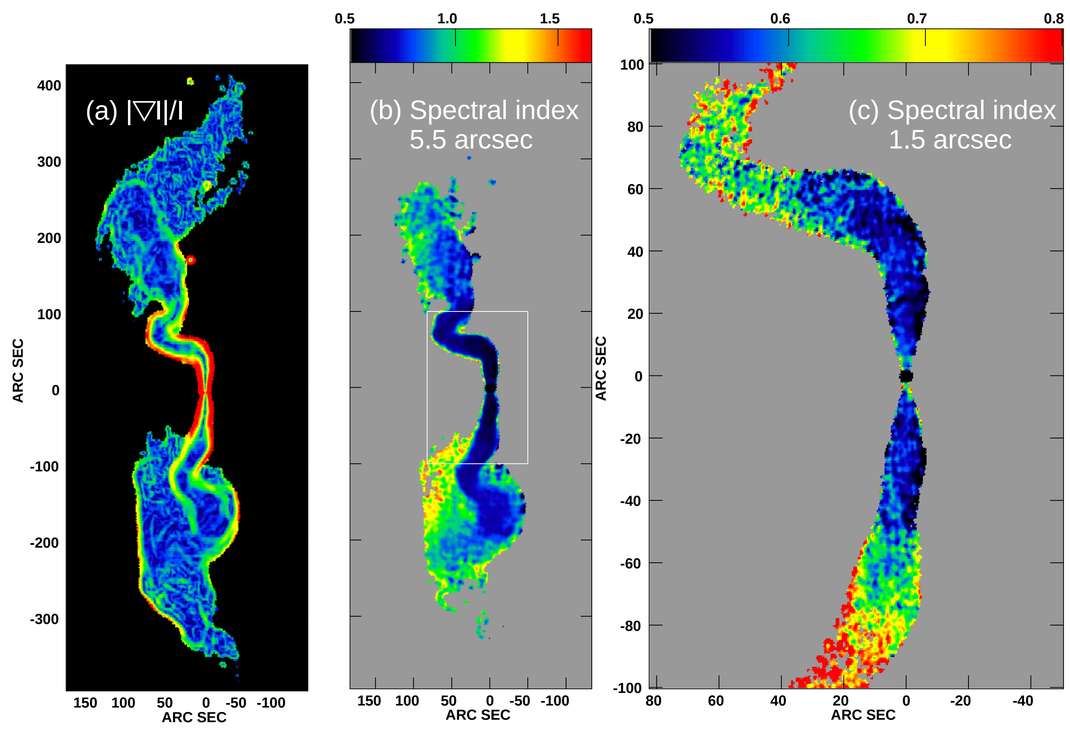

Figure 3: Radio images of 3C 31. (a) Sobel-filtered, mean L-band image (normalized by total intensity) at a resolution of 5.5 arcsec. (b) and (c) Spectral index, α from weighted least-squares, power-law fits to the total intensity. (b) 5-frequency fit between 1365 and 4985 MHz at a resolution of 5.5 arcsec FWHM. (c) 6-frequency fit at a resolution of 1.5 arcsec FWHM for the inset area in panel (b).

4 Radio and X-ray profiles

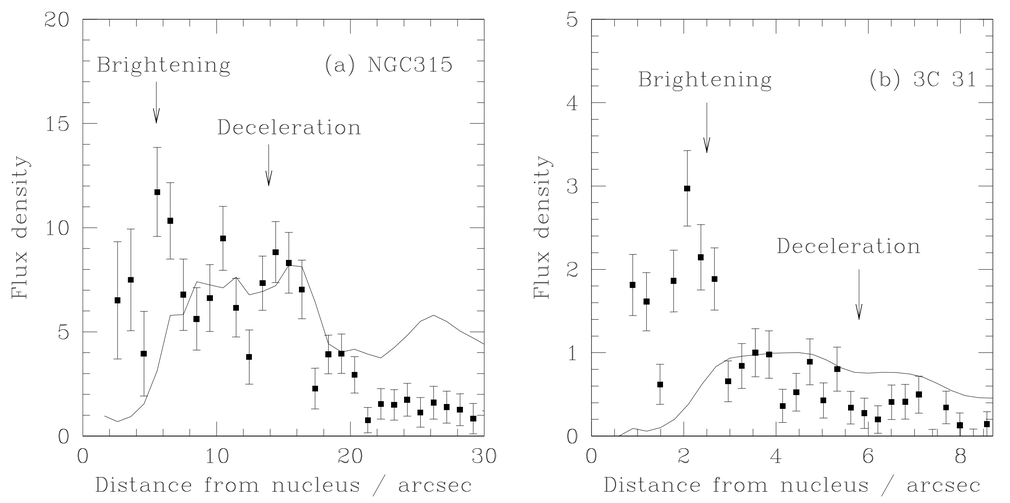

Figure 4: Profiles of radio (curve) and X-ray (points) flux density along the brighter jet of NGC 315 [13]. The locations of the brightening point (where the rest-frame radio emission increases rapidly) and the start of rapid deceleration, as modelled by [1] are also indicated.

Figure 5: Profiles of radio (curve) and X-ray (points) flux density along the brighter jet of 3C 31, as in Fig. 4 [2,5,6].

5 3C 296

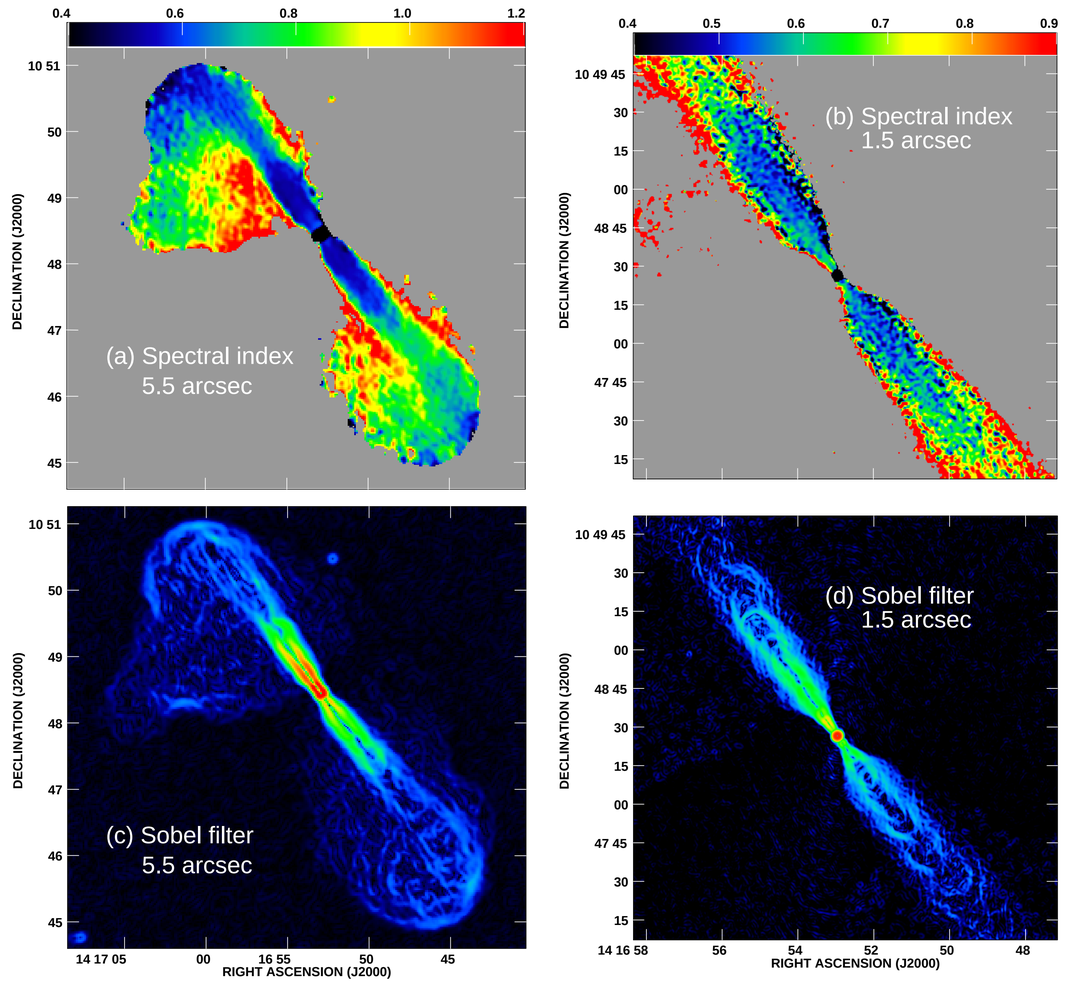

Figure 6: False-colour plots of spectral index and intensity gradients for 3C 296 [8]. (a) Spectral index between 1.48 and 8.5 GHz at a resolution of 5.5 arcsec FWHM. (b) Spectral index between 1.4 and 8.5 GHz at a resolution of 1.5 arcsec FWHM. (c) Sobel-filtered L-band image at 5.5 arcsec FWHM; (d) Sobel-filtered 8.5-GHz image at 1.5 arcsec FWHM.

6 Discussion

These observations contribute to the developing picture of spectral variations in FR I sources, as follows.

- Bright X-ray emission is detected close to the nucleus, in the faint, well-collimated jet bases that precede the sudden radio brightening (Figs 2b, 4, 5).
- There is approximate morphological correspondence between features in the radio and X-ray brightness distributions after the former brightens, although there are differences on small scales (e.g. Fig. 2b). There are no systematic transverse variations in the X-ray/radio ratio within ≈30 arcsec of the nucleus in NGC 315 (the best resolved case [13]). Particle acceleration appears to be distributed throughout the jet volume, rather than being exclusively associated with discrete knots or with the boundary.
- The ratio of X-ray to radio emission decreases where our kinematic models show that the jets start to decelerate from speeds of $0.8 - 0.9c$ (Figs 4 and 5; [1, 5]).
- Where the jets first brighten and before they decelerate, there is a remarkably small dispersion around a radio spectral index of $\alpha = 0.62$ in the three sources we have studied in detail (Figs 1b, 3c, 6b). The average is dominated by emission immediately after the point at which the jets first brighten. This is also the region from which X-ray emission is detected from the main jets in all three sources (Figs 4 and 5; [3]).
- The spectral index of the fainter emission close to the nucleus in 3C 449 [11] and PKS1333−33 [4] appears to be comparable to or slightly steeper than $\alpha = 0.62$ although the uncertainties are larger.
- Further from the nucleus, the spectra flatten slightly to $\alpha = 0.50 - 0.55$. X-ray emission is still detected from these regions, but at a lower level relative to the radio (Figs 4 and 5).
- The brightest X-ray emission from the jets is therefore not associated with the flattest radio spectra, but rather with some particle acceleration process whose characteristic energy index is $2\alpha + 1 = 2.24$.
- A related result is that an asymptotic low-frequency spectral index of 0.55 is common in FR I jets over larger areas than we consider here [14].
- Flatter-spectrum edges can be seen where the jets are isolated from significant surrounding diffuse emission, most clearly in NGC 315 (Fig. 1a). Our kinematic models [1, 5, 8] show that all of the jets have substantial transverse velocity gradients and it is plausible that the process that produces the flatter spectrum is associated with high shear [10, 12]. In 3C 31, the flatter-spectrum regions (Fig. 3c) occur predominantly on the W edges of the jets, i.e. on the outer edges of bends, perhaps consistent with this idea.
- As well as a smooth steepening of the jet spectrum at larger distances from the nucleus, as would be expected from synchrotron and adiabatic losses affecting a homogeneous electron population, multiple spectral components are observed (Figs 3b and 6a). Jets appear to retain their identities even after entering regions of diffuse emission and are clearly identifiable by their flatter spectra. They are usually also separated from the surrounding emission by sharp brightness gradients (Figs 3a and 6c).
- This spine/sheath separation is observed in FR I sources with bridges of emission extending back towards the nucleus (e.g. 3C 296; Fig. 6) as well as tailed sources like 3C 31 (Fig. 3). Although there is an overall trend for the spectrum of the diffuse emission to steepen towards the nucleus in bridges and away from it in tails [9], the variations in individual objects such as 3C 31 are complex.
- The termination regions of jets in tailed FR I sources are perhaps best regarded as bubbles which are continually fed with fresh relativistic plasma by the jets and which in turn leak material into the tails. Their spectral steepening would then be governed by a combination of continuous injection, adiabatic, synchrotron and inverse Compton energy losses and escape.

[1] Canvin, J.R., Laing, R.A., Bridle, A.H., Cotton, W.D., 2005, MNRAS, 363, 1223
[2] Hardcastle, M.J., Worrall, D.M., Birkinshaw, M., Laing, R.A., Bridle, A.H., 2002, MNRAS, 334, 182
[3] Hardcastle M.J., Worrall D.M., Birkinshaw M., Laing R.A., Bridle A.H., 2005, MNRAS, 358, 843
[4] Killeen N.E.B., Bicknell G.V., Ekers R.D., 1986, ApJ, 302, 306
[5] Laing, R.A., Bridle, A.H., 2002, MNRAS, 336, 328
[6] Laing, R.A., Bridle, A.H., 2004, MNRAS, 348, 1459
[7] Laing R.A., Canvin J.R., Cotton W.D., Bridle A.H., 2006, MNRAS, 368, 48
[8] Laing, R.A., Canvin, J.R, Bridle, A.H. Hardcastle, M.J., 2006, MNRAS, 372, 510
[9] Parma, P., Murgia, M., Morganti, R., Capetti, A., de Ruiter, H.R., Fanti, R., 1999, A&A, 344, 7
[10] Rieger, F.M., Duffy, P., 2006, ApJ, 652, 1044
[11] Rudnick, L., Katz-Stone, D.M., 1997, ApJ, 488, 146
[12] Stawarz, L., Ostrowski, M., 2002, ApJ, 578, 763
[13] Worrall, D.M., Birkinshaw, M., Laing, R.A., Cotton, W.D., Bridle, A.H., 2007, MNRAS, in press
[14] Young A., Rudnick L., Katz D., Delaney T., Kassim N.E., Makishima K., 2005, ApJ, 626, 748